Research Square

Preprints are preliminary reports that have not undergone peer review.
They should not be considered conclusive, used to inform clinical practice,
or referenced by the media as validated information.

Physicochemical Characteristics of the Great Kwa River (Gulf of Guinea): Controls of Tidal Dynamics and Environmental Sustainability in a Tropical Mesotidal System

Chimezie Ndunagum Emeka
emekachimezie@unical.edu.ng
University of Calabar
Victoria Inyang Emeka
University of Calabar
Asukwo Essien Itam
University of Calabar
Bassey Offiong Ekpo
University of Calabar
Lailah Gifty Akita
University of Ghana
Benjamin Odey Omang
University of Calabar
Celsus Adie Agim
University of Calabar
Aniekan Clement Ukpe
University of Calabar
Samuel Augustine Ikpe
University of Calabar
Etie Ben Akpan
University of Calabar

Research Article

Keywords: Great Kwa River, tidal dynamics, physicochemical characteristics, hydro-physicochemical facies, Gulf of Guinea

Posted Date: May 27th, 2026

DOI: https://doi.org/10.21203/rs.3.rs-9595578/v1

License: This work is licensed under a Creative Commons Attribution 4.0 International License. Read Full License

Additional Declarations: No competing interests reported.

Abstract

The physicochemical characteristics of the Great Kwa River, a tidal tributary of the Cross River estuary (Gulf of Guinea), were investigated to evaluate water quality, hydrodynamic controls, and implications for environmental sustainability in a tropical meso-tidal system. Fifty bottom-water samples were collected along a 17.65 km tidal reach and analysed in-situ for temperature, pH, salinity, electrical conductivity, turbidity, and transparency, alongside measurements of tidal current velocity and bathymetry. Results indicate a semi-diurnal, ebb-dominated tidal regime, with current asymmetry driven by the interaction between tidal forcing and fluvial discharge. Physicochemical parameters show narrow ranges: temperature (25–28°C), pH (6.0–7.5), salinity (0.014–0.039‰), electrical conductivity (20–58 µS/cm), and transparency (0.3–1 m), all within acceptable limits for freshwater systems. A clear downstream gradient is observed, characterized by increasing salinity and conductivity, and decreasing temperature and pH, reflecting progressive tidal influence and limited estuarine mixing during the study period. Three hydro-physicochemical facies were delineated: (i) an upper fluvial-dominated facies with low salinity and high transparency, (ii) a middle transitional facies exhibiting maximum variability and sediment reworking, and (iii) a lower tidally influenced facies marked by elevated salinity and enhanced fine sediment deposition. Strong correlations among salinity, conductivity, and total dissolved solids highlight the role of ionic concentration in controlling water chemistry, while turbidity patterns reflect localized sediment resuspension linked to channel morphology and flow convergence. The study demonstrates that hydrodynamic processes exert fundamental control on physicochemical distribution and sedimentary facies organization in the river. Despite its current freshwater status and ecological suitability, the system shows early sensitivity to anthropogenic and hydrological changes. In this context, environmental sustainability implies proactive monitoring, sediment regulation, and pollution control to preserve the river's ecological integrity and ensure its continued role as a resilient freshwater resource for Calabar and the wider Gulf of Guinea.

1. Introduction

Tidal rivers are characteristic features of meso- to macro-tidal environments and are generally absent in microtidal settings where wave processes dominate hydrodynamics. They are commonly defined as naturally occurring, channelized water bodies that experience periodic tidal fluctuations, possess a freshwater source at their headwaters, and discharge into estuarine systems at their mouths without direct open-ocean exposure (Antia et al., 2012; Emeka et al., 2010; C. N. Emeka et al., 2024b; C. N. Emeka, V. I. Emeka, E. D. Ebong, et al., 2023). Functionally, tidal rivers represent transitional zones within the land–sea continuum, where fluvial and estuarine processes interact to produce distinct hydrodynamic, sedimentological, and physicochemical regimes.

The physicochemical characteristics of tidal rivers are strongly controlled by the interplay between river discharge and tidal forcing, including flood, ebb, and slack-water conditions. These processes regulate mixing intensity, sediment resuspension, and the spatial distribution of dissolved and particulate constituents. The degree of tidal penetration inland plays a critical role in determining salinity gradients, ionic composition, and overall water quality (Uncles, 2002; Winterwerp & van Kesteren, 2004). In many tropical mesotidal systems, ebb dominance—driven by fluvial input and tidal asymmetry—enhances downstream transport of sediments and limits saline intrusion, thereby maintaining predominantly freshwater conditions in upstream reaches (Dyer et al., 2004; Emeka et al., 2010; C. N. Emeka et al., 2024a, 2024b; V. I. Emeka, C. N. Emeka, E. Agi-Odey, et al., 2024; V. I. Emeka, C. N. Emeka, A. E. Itam, A. Ambo, et al., 2024; V. I. Emeka, C. N. Emeka, A. E. Itam, & E. E. Nyong, 2024). These dynamics are critical in shaping the physicochemical structure and ecological functioning of tidal river environments.

Key physicochemical parameters such as transparency, turbidity, temperature, pH, electrical conductivity (EC), salinity, and total dissolved solids (TDS) serve as fundamental indicators of water quality and environmental health. Transparency and turbidity reflect suspended sediment concentrations and influence light penetration and primary productivity (World Health Organization, 2017, 2022). Water temperature governs biochemical reactions and microbial activity, while pH regulates chemical stability and biological processes within aquatic systems. Electrical conductivity, salinity, and TDS provide measures of dissolved ionic content, integrating both natural geological controls and anthropogenic inputs such as urban runoff and industrial discharge (Hem, 1985; Winterwerp & van Kesteren, 2004). Variations in these parameters are therefore essential for understanding both the natural dynamics and environmental sustainability of tidal river systems.

The Great Kwa River, a major tributary of the Cross River estuary in southeastern Nigeria, originates from the Oban Hills in central Cross River State, and flows southwards into the Cross River estuary, along the southeast coast of Nigeria (Fig. 1). The river traverses diverse geological formations, including Precambrian Basement Complex rocks, Cretaceous sediments of the Calabar Flank, and younger Coastal Plain Sands. It is of considerable socio-economic importance, serving as a primary source of potable water for Calabar and adjacent communities, while also supporting navigation, sand mining, and coastal infrastructure development. Increasing anthropogenic pressures within the basin raise concerns regarding water quality deterioration and long-term environmental sustainability.

This study investigates the physicochemical characteristics of the lower reaches of Great Kwa River within a tropical mesotidal setting, with particular emphasis on the role of tidal dynamics in controlling water quality patterns. Parameters including Secchi disc transparency, turbidity, temperature, pH, electrical conductivity, salinity, and total dissolved solids were analyzed to evaluate spatial variability and environmental conditions within the channel. The study provides baseline data for assessing anthropogenic impacts and contributes to a broader understanding of the linkages between tidal processes, water chemistry, and environmental sustainability in tropical tidal river systems.

2. Methodology

Tidal current velocities of the Great Kwa River were measured in the rainy season months of August and September 2020, while the channel was mapped in September 2020. Parameters studied include bathymetry and water quality parameters (pH, temperature, turbidity and salinity). Tidal current velocity was measured at two stations over Spring, Mean, and Neap tidal cycles. Depth soundings, turbidity measurements, and water samples were simultaneously obtained from the same georeferenced stations within the studied channel, as shown in Fig. 2.

2.1 Measurement of tidal current velocity

Surface tidal current velocity and direction were measured at two stations along the western bank of Great Kwa River namely, Obufa Esuk Orok (OEO) and Esuk Mba (EM). Readings were obtained at Spring, Mean, and Neap Tide.

The Langrangian method was used for this study. It involves the use of a stopwatch to measure the time it takes a floating object in the channel to traverse a pre-measured distance (preferably 10m) parallel to the channel. This procedure was repeated thrice every 15 minutes for 12 hours per day, and direction of flow was obtained using a Brunton Compass. Tidal current velocity (v) was obtained by dividing the distance travelled (x) by the average drift time (t') for every 15-minute interval (Eq. 1) at both ebb and flood tide.

$$V = \frac{x}{t\prime}$$

1

2.2 Depth sounding

A total of 50 sample stations were established in Great Kwa River, using a portable Garmin global positioning system. Depth soundings were made at these stations using a portable single beam echo sounder.

2.3 Secchi disc transparency

Transparency readings were obtained simultaneously with depth sounding, using a Secchi disc. This was done by dipping the disc into water at each geo-referenced station until it just disappeared. The depth at which this happened was obtained by measuring the length of the rope, from the disc-to the water mark at the point of disc disappearance. The recorded in a notebook.

2.4 Bottom water sampling and physicochemistry

Fifty bottom water samples were obtained from the channel, using a Nansen water sampler, simultaneously with depth sounding and turbidity measurement. These samples were analysed in-situ for physicochemical parameters (pH, electrical conductivity, salinity and temperature), using a HANNA hand-held combo pH/EC/TDS/Temperature meter (HI 98130), by dipping it into a cup containing the sample. The corresponding values were read off its screen, after they had stabilized.

Turbidity was measured using a Hanna Instruments HI 93703 Portable Turbidimeter/Nephelometer. This was done in-situ by filling a clean cuvette up to a quarter inch from its rim and agitating it. The bubbles in the water were allowed to escape, after which the cap of the cuvette was secured. It was then placed into the cell of the meter, with the notch on the cap positioned securely into the groove, and the mark on the cuvette pointed towards the LCD. The read key on the device was pressed, after which a blinking "SIP" (Sampling in Process) message displayed on the screen. The turbidity value appeared approximately 20 seconds after.

3. Results

3.1 Hydrodynamics

Results of the tidal current velocity measurements for Great Kwa River are presented in Fig. 3 and Table 1. The highest velocities occurred at Spring Ebb (84 cm/s) clearly showing ebb-dominance (Table 1). Water waves in Great Kwa River were generated by wind, and water transport vessels, and were generally insignificant.

3.2 Bathymetry

The bathymetry map and sections of the studied segment of Great Kwa River, as presented in Figs. 4, were produced relative to mean tide low water slack (MTLWS). The channel was relatively shallow, with an average depth of 2.8 m ± 1.9 m, and maximum depth of 7 m (Fig. 4a, Table 2). The shallowest parts of the channel were located towards the upstream segment, while the downstream segment bore the deepest portions. The cross-channel section (Fig. 4b) showed that the channel was deepest in the mid channel and shallowest at the banks, the west bank being generally shallower than the east bank. Figure 4c is a linear trend of the along channel cross-sectional profile (Fig. 4d) of the studied segment. It shows a downstream deepening trend.

3.3 Transparency

The distribution of transparency within Great Kwa River is presented in Fig. 5a. Turbidity values varied between 26 cm and 106 cm, with an average of 68.28 cm ± 16.6 cm (Table 2). The least transparent part of the channel occurred around the sand bar at the central segment of the channel, with values ranging from 20 cm to 80 cm. The upstream segment had the clearest water, with values between 60 cm and 106 cm. The downstream area had transparency values between 60 cm and 80 cm. Transparency significantly moderately positively correlated with depth in the channel (Table 3)

3.4 Turbidity

Turbidity values within the channel ranged from 1.51 and 12.71 NTU (Table 2), clearly demarcating the channel into three zones (Fig. 5b). The upper zone, which extended from the upper limit of the study area to the upper end of the central tidal bar, was the clearest part of the channel (1–5 NTU). The central zone was the most turbid, with variegated turbidity values between 1–13 NTU. The lower zone had turbidity values between 1 and 8 NTU, making it more turbid than the upper zone, but less than the central zone. Turbidity significantly weakly positively correlated with electrical conductivity, salinity, salinity, and

total dissolved solids (Table 3). It also significantly negatively correlated with depth and Secchi disc transparency, moderately and strongly, respectively (Table 3).

3.5 Temperature

The distribution of bottom water temperature within Great Kwa River is presented in Fig. 5c. Temperatures varied between 25°C and 28°C, having an average value of 26.4°C ± 1.03°C (Table 2). In the upstream segment, the channel had a predominant temperature range of 26°C to 28°C and was principally 25°C to 26°C downstream, effectively having a downstream cooling trend. Bottom water temperature within the channel had a non-significant weak negative correlation with depth and no correlation with turbidity (Table 3).

3.6 pH

The distribution of bottom water pH within Great Kwa River is presented in Fig. 5d. pH values within the channel ranged from slightly acidic to slightly alkaline (6 to 7.5) and were averagely neutral (6.9 ± 0.4) (Table 2). There was an even distribution of slightly acidic to neutral (6.5 to 7) and neutral to slightly alkaline (7 to 7.5) bottom waters all through the channel. However, slightly acidic waters (6 to 6.5) occur as large patches in the downstream segment of the channel. The distribution of pH within the channel showed a downstream decreasing trend. pH had non-significant, weak, negative correlations with depth and turbidity but a significant positive correlation with temperature within the channel (Table 3).

3.7 Electrical Conductivity

The distribution of Electrical Conductivity within the Great Kwa River is presented in Fig. 6a. The map shows a dominant conductivity of 20–30 µS/cm in the upstream segment of the channel. The central segment was dominated by a mix of 30–40 µS/cm, while the downstream segment of the channel was predominantly 40–50 µS/cm. The Descriptive statistics of Electrical conductivity within the Great Kwa River is shown in Table 2. Electrical conductivity had significant weak negative correlations with Secchi disc transparency and turbidity, while it had perfect correlations with salinity and total dissolved solids (Table 3).

3.8 Salinity

The distribution of bottom water salinity within Great Kwa River is presented in Fig. 5d. Salinity values within the channel ranged from 0.014‰ to 0.039‰, indicating a freshwater tidal channel. The average salinity value within the channel was 0.021‰ ± 0.005‰ (Table 2). Salinity progressively increased downstream within the channel. Salinity had non-significant weak negative correlations with depth and temperature, but a significant negative correlation with turbidity (Table 3).

3.9 Total Dissolved Solids (TDS)

TDS within the channel ranged from 12.1 ppm to 31.9 ppm (Table 2). In Fig. 6a, a clear demarcation of the of the channel into 3 zones is shown, based on TDS. A downstream increasing trend in TDS concentration is observed, with the upstream zone having the least values (10–15 ppm), and the downstream segment having the highest values (20–35 ppm). TDS significantly weakly negatively correlated with secchi dsic transparency, and positively with turbidity (Table 3).

3.10 Hydro-Physicochemical Facies Associations

Three facies were delineated within the channel, based on the physicochemical properties of the river (Fig. 6). The Upper Facies was the most distal from the estuary and occurred towards the head of the channel. It was straight, occupied an area of 1.41 km^2, covered a stretch of 2.76 km and had a maximum depth of 5.2 m, with dominant depth ranges of 1 to 2 m, 2 to 3 m, and 3 to 4 m. It had a maximum turbidity of 106 cm, with dominant ranges of 60 to 80 cm, and 80 to 100 cm. The maximum temperature in this section was 28°C, with dominant temperature ranges of 26 to 27°C and 27 to 28°C. The maximum pH of this section was 7.4, with a dominant range of 6 to 7. Salinity within this segment of the channel ranged from 0.014‰ to 0.019‰, making it the segment of the channel with the least salinity. The least salinity value here was 0.01408‰.

The Middle Facies was 10.16 km long, covered an area of 6.96 km^2, and had a maximum depth of 6.6 m. Depth within this segment increased in a downstream direction, with depth ranges of 1 m to 2 m, and 2 m to 3 m dominating upstream, while 3 m to 4 m, and 4 m to 5 m dominating downstream. The dominant turbidity within this segment was 60 cm to 80 cm. The most turbid part of this section was towards the western bank of its central portion, where turbidity ranged between 20 cm and 60 cm. The least turbid area occurred upstream, as small patches of 80 cm to 100 cm turbidity. Bottom water temperature within this section generally cooled in the downstream direction, with temperatures values of 27°C to 29°C occurring exclusively upstream. The dominant temperature ranges of the facies were 26°C to 27°C, and 25°C to 26°C. pH ranged between 6 to 7, and 7 to 8 in the upstream region, while the downstream area was predominantly composed of a pH range of 6 to 7. Salinity gradually increased in the downstream direction, with this facies. It predominantly ranged between 0.019‰ and 0.024‰, with ranges of 0.014‰ to 0.019‰, and 0.024‰ to 0.029‰ featuring prominently upstream and downstream, respectively.

The Lower Facies occurred towards the mouth of the channel and was the most proximal to Cross River estuary. It covered a stretch of 4.73 km, and an area of 3.49 km^2. The dominant depth range within this segment was 2 m to 3 m, and the maximum depth was 5.9 m. Turbidity dominantly ranged between, 60 cm and 80 cm, with a smaller turbid area of 40 cm to 60 cm, occurring upstream. Temperature was dominantly between 25°C and 26°C. pH, in equal proportions, ranged from 7 to 8, upstream, and 6 to 7, downstream. Based on salinity, the Lower Facies association was divided into three subfacies. The upstream subfacies was composed predominantly of a salinity range of 0.029‰ and 0.034‰, with a minor occurrence of 0.034‰ and 0.039‰. The central subfacies occupied 70% of the Lower Facies association and was 90% composed of a salinity range between 0.024‰ and 0.029‰. The lower sufacies was exclusively composed of a salinity range of 0.029‰ and 0.034‰.

Table 1: Maximum flood and ebb-tidal current velocities in Great Kwa River

Tidal Cycles	Flood current velocity (cm/s)		Ebb current velocity (cm/s)	
	Obufa Esuk Orok	Esuk Mba	Obufa Esuk Orok	Esuk Mba
Spring	68	76	81	84
Mean	61	66	75	78
Neap	49	58	61	64

Table 2
Descriptive statistics of Great Kwa River physicochemistry

N	Depth (m)	Secchi disc transparency (cm)	Turbidity (NTU)	Water temp (ºC)	pH	Electrical conductivity (µS/cm)	Salinity (‰)	TDS (ppm)
	50	50	50	50	50.00	50	50	50
Min	0.9	26	1.51	25	6.00	22	0.01408	12.1
Max	7	106	12.71	28	7.50	58	0.03712	31.9
Mean	2.8	68.28	5.3138	26.4	6.90	33.5	0.02144	18.425
Std. error	0.2671	2.3455	0.3336	0.1457	0.06	1.1892	0.0008	0.6540
Variance	3.5673	275.0629	5.5632	1.0612	0.15	70.7041	2.90E-05	21.3880
Stand. dev	1.8887	16.5850	2.3586	1.0302	0.39	8.4086	0.0054	4.6247
Median	1.6	70	4.82	26	6.90	30.5	0.0195	16.7750
Geom. mean	2.2404	65.7904	4.8993	26.3803	6.88	32.5478	0.0208	17.9013
Coeff. var	67.4551	24.2897	44.3871	3.9021	5.70	25.1002	25.1002	25.1002
World Health Organization (2011, 2022)			1		6.5–8.5			600
Nigerian Industrial Standard, (2007, 2015)			5	Ambient	6.5–8.5	1000		500

Table 3: Pearson moment correlation of Great Kwa physicochemistry

(a) Coefficient of correlation (r)

	Depth (m)	Secchi disc transparency (cm)	Turbidity (NTU)	Water temp (□C)	pH	Electrical conductivity (µS/cm)	Salinity (
Secchi disc transparency (cm)	0.497						
Turbidity (NTU)	-0.475	-0.982					
Water temp (□C)	-0.233	0.010	-0.023				
pH	-0.262	-0.104	0.102	0.332			
Electrical conductivity (µS/cm)	-0.153	-0.360	0.310	-0.231	-0.011		
Salinity (‰)	-0.153	-0.360	0.310	-0.231	-0.011	1	
TDS (ppm)	-0.153	-0.360	0.310	-0.231	-0.011	1	

(b) Probability of significance (P)

	Secchi disc transparency (cm)	Turbidity (NTU)	Water temp (□C)	pH	Electrical conductivity (µS/cm)	Salinity (‰)	TDS
Depth (m)	0.00024	0.00049	0.10367	0.06588	0.29029	0.29029	0.
Secchi disc transparency (cm)		3.14E-36	0.94487	0.47300	0.01020	0.01020	0.
Turbidity (NTU)			0.87642	0.48018	0.02829	0.02829	0.
Water temp (□C)				0.01854	0.10670	0.10670	0.
pH					0.94228	0.94228	0.
Electrical conductivity (µS/cm)						1.92E-234	1.92
Salinity (‰)							1.92

* Highlighted data are significant at $p \leq 0.05$

4. Discussion

4.1 Tidal Processes

The Great Kwa River exhibits a mesotidal, semi-diurnal regime (Fig. 3; Table 1), consistent with tidal systems along the southeastern Nigerian coast (Davies, 1964; Flemming, 2012; Hayes, 1979; Nigerian Navy, 2018; Sexton & Murday, 1994). The observed ebb dominance reflects strong tidal–fluvial coupling, where river discharge enhances ebb velocities and promotes net seaward sediment transport. This asymmetry has been reported in coastal channels proximal to the Great Kwa River (Antia et al., 2012; Emeka et al., 2010; C. N. Emeka et al., 2024a, 2024b; C. N. Emeka, V. I. Emeka, E. K. Agi-Odey, et al., 2023; C. N. Emeka, V. I. Emeka, E. B. Akpan, et al., 2023; C. N. Emeka, V. I. Emeka, E. D. Ebong, et al., 2023; V. I. Emeka et al., 2023; V. I. Emeka, C. N. Emeka, A. E. Itam, A. Ambo, et

al., 2024) and is widely reported in tide-influenced channels and is a primary mechanism controlling sediment export and channel morphodynamics (Dalrymple et al., 2012; Davis & Dalrymple, 2012; Gong et al., 2016; Guo, 2014; Guo et al., 2014; Li & Gong, 2016; Uncles, 2002).

The weak wave climate indicates that hydrodynamics is primarily current-driven rather than wave-dominated. Consequently, sediment transport and bedform development are governed by tractional processes, including ripple migration and channel scouring. Similar conditions have been reported in tropical mesotidal estuaries where tidal currents dominate over wave energy (Asp et al., 2018; C. N. Emeka, V. I. Emeka, E. D. Ebong, et al., 2023; V. I. Emeka et al., 2023; Freitas et al., 2012).

Bathymetric characteristics (Fig. 6) further confirm tidal control. The downstream increase in depth and concentration of maximum depths along the thalweg reflect enhanced tidal scouring, lateral accretion along channel margins, and increasing accommodation space toward the estuary. These features are typical of tidally influenced fluvial systems undergoing downstream hydraulic adjustment (Asp et al., 2018; Whitehouse et al., 2000)

4.2 Hydrochemistry

4.2.1 Salinity, Electrical Conductivity, and Total Dissolved Solids

The extremely low salinity range (0.014–0.039‰) (Table 4) indicates negligible marine intrusion during the study period, classifying the system as freshwater-dominated despite tidal influence. This is attributed to high freshwater discharge during the rainy season, which suppresses saline penetration (C. N. Emeka, V. I. Emeka, E. K. Agi-Odey, et al., 2023).

The progressive downstream increase in salinity, conductivity, and TDS (Table 4) reflects incipient estuarine mixing. The strong correlation among these parameters is consistent with their shared dependence on ionic concentration (Hem, 1985; Rahman et al., 2022). Compared to the Calabar River, Cross River estuary and Qua-Iboe River estuaries, the Great Kwa River shows significantly lower salinity values, likely due to differences in channel morphology, tidal exchange efficiency, and anthropogenic disturbance (C. N. Emeka et al., 2024a, 2024b; C. N. Emeka, V. I. Emeka, E. K. Agi-Odey, et al., 2023).

4.2.2 Temperature

The downstream decrease in temperature (Table 4) reflects increased mixing, depth-related heat distribution, and reduced solar heating due to turbidity. Such trends are typical of well-mixed tidal rivers where stratification is weak (Geyer & MacCready, 2014; MacCready et al., 2018; Uncles, 2002).

4.2.3 pH Distribution

The near-neutral pH (6.0–7.5) of the Great Kwa River indicates a well-buffered system controlled by carbonate equilibria and organic matter decomposition. The slight downstream decrease in pH suggests increased microbial respiration and CO_2 production toward the estuarine interface (Kaselowski & Adams, 2013). The pH of the Great Kwa River falls within the permissible limits of portable water. Pure water has a pH of 7.00 at 25°C (Hem, 1985). The permissible limits of pH in portable water as 6.5 to 8.5 (World Health Organization, 2011, 2022).

4.2.4 Secchi Disc Transparency and Turbidity

Transparency and Turbidity distributions (Fig. 6a and 6b; Table 4) show localized minima and maxima (respectively) at the central sand bar, reflecting sediment resuspension due to flow convergence and turbulence. The positive and negative relationships between transparency and turbidity, and depth (respectively) suggests that deeper sections sustain stronger currents capable of maintaining suspended sediments (Dijkstra et al., 2018; Ubuoh et al., 2024; Winterwerp, 2007; Winterwerp & Wang, 2021).

Overall, the hydrochemical regime reflects a tidally mixed freshwater system transitioning toward estuarine conditions, with strong coupling between physical and chemical processes.

4.3 Environmental Sustainability

The physicochemical conditions (Table 4) indicate a relatively stable and ecologically supportive estuarine system. Observed near-neutral pH and moderate tropical temperatures (≈ 25–30°C) are consistent with conditions reported for the Cross River estuary, where warm, shallow waters promote biological productivity and regulate dissolved oxygen dynamics. The predominance of low salinity (oligohaline conditions) reflects strong fluvial influence and favours freshwater to brackish biodiversity typical of the upper and middle estuarine zones (Otogo et al., 2021; Ukpong et al., 2015).

However, localized environmental concerns include: elevated turbidity zones (Fig. 6), or turbidity maxima zones, which may reduce light penetration and primary productivity (Burchard et al., 2004; Grasso et al., 2025), slight downstream acidification, possibly linked to organic loading, and Increasing conductivity, which may indicate early-stage contamination or estuarine influence

Given the hydrological connectivity of the Great Kwa River to the Cross River estuary, it is susceptible to saline intrusion, particularly under conditions of reduced freshwater discharge when tidal forces become dominant. This vulnerability is further intensified by anthropogenic disturbances such as channel dredging and increased urban runoff, which alter hydrodynamic regimes, enhance saltwater penetration, and degrade water quality (Matsoukis et al., 2022; Odigie & Obayagbona, 2025).

Sustainable management should prioritize continuous monitoring of salinity intrusion, regulation of upstream inputs, and control of sediment disturbance.

4.4 Facies Differentiation

The longitudinal variation in physicochemical parameters (Table 4) defines three distinct hydro-physicochemical facies, consistent with classical estuarine models (Dalrymple et al., 1992).

Table 4
Integrated downstream trend

Parameter	Upper Facies (Distal)	Middle Facies (Transitional)	Lower Facies (Proximal)
Salinity	Lowest	Increasing	Highest
Depth	Moderate	Highest	Moderate
Turbidity	Highest clarity	Moderate	Moderate
Temperature	Highest	Decreasing downstream	Lowest
pH	Neutral	Variable	Slightly higher

4.4.1 Upper Facies (Fluvial-Dominated)

This facies is characterized by low salinity, shallow water depth, high water transparency, and near-neutral pH (Fig. 7; Table 4), indicating strong fluvial dominance within the upper estuarine reach. Such conditions are typical of high-energy river-influenced zones, where increased flow velocity promotes sediment entrainment and transport. In these settings, sediments are commonly dominated by fine- to medium-grained sands, mobilized primarily through tractional processes such as rolling and saltation along the channel bed. Consequently, this zone functions largely as a sediment transport pathway with minimal net deposition, consistent with hydrodynamic sorting and sediment bypass observed in upper estuarine environments (Dalrymple et al., 1992; Nichols, 2009; Reineck & Singh, 1986).

4.4.2 Middle Facies (Transitional Zone)

The middle facies (Fig. 7; Table 4) is characterized by greater water depth and pronounced variability in physicochemical parameters, reflecting its position within the fluvial–estuarine transition zone where riverine and marine processes interact. These fluctuating hydrodynamic conditions promote the development of heterolithic facies, expressed as alternating sand–mud successions typical of tidally influenced environments. Increasing salinity within this transitional zone enhances the flocculation of fine-grained suspended sediments, leading to the formation of larger aggregates with higher settling velocities. This process contributes to the development of an estuarine turbidity maximum (ETM), a zone of elevated suspended sediment concentration that functions as a dynamic and temporary sediment sink within the estuary (Abascal-Zorrilla et al., 2020; Abril et al., 2000; Burchard et al., 2004; Dyer et al., 2004; Geyer & MacCready, 2014; Grasso et al., 2025; MacCready et al., 2018; Park et al., 2008; Uncles et al., 2006).

4.4.3 Lower Facies (Tidally Influenced)

This facies is characterized by the highest salinity and relatively stable turbidity (Fig. 7; Table 4), reflecting a stronger marine and tidal influence within the estuarine system. Under such conditions, reduced current velocities during slack water, coupled with increased salinity-driven flocculation of suspended particles, enhance the settling of fine-grained sediments. Consequently, the deposits are typically mud-dominated, often exhibiting laminated structures and tidal rhythmites, which are indicative of cyclic tidal deposition and mark this zone as a major sedimentary sink within the estuary (Dalrymple et al., 1992; Dyer et al., 2004; Nichols, 2009; Winterwerp, 2007). This is supported by the results of C. N. Emeka, V. I. Emeka, E. D. Ebong, et al. (2023), who showed that this part of the channel was predominantly composed of mud.

4.5 Sedimentological Significance

Results from this study indicate that hydrodynamic and hydrochemical processes play a fundamental role in controlling sediment transport pathways and the development of facies architecture in estuarine environments. In particular, ebb-dominated tidal regimes enhance net seaward sediment transport, leading to channel deepening and incision, as well as the preferential export of fine-grained sediments from the estuary to the adjacent shelf (Allen et al., 1980; Aubrey, 1986; Burchard et al., 2018; Ginsberg & Aliotta; Winterwerp et al., 2013).

Therefore, the system is expected to exhibit a classical downstream facies succession (Fig. 7; Table 4): sandy fluvial facies (Upper), heterolithic transitional facies (Middle), and mud-dominated estuarine facies (Lower). This is supported by results obtained in the sedimentological study of the Great Kwa River by C. N. Emeka, V. I. Emeka, E. D. Ebong, et al. (2023), and corresponds to the model of (Dalrymple et al., 1992).

Salinity gradients play a critical role in estuarine sediment dynamics by promoting flocculation of suspended particles, thereby enhancing the settling and deposition of fine-grained sediments. Variations in water depth further influence hydrodynamic energy conditions and the availability of accommodation space, which together control sediment transport pathways and depositional patterns. Turbidity, as an indicator of suspended sediment concentration, reflects both sediment load and the efficiency of transport processes within the estuarine system (Dalrymple, 2010; Winterwerp, 2007; Winterwerp et al., 2013)

The middle estuarine facies represents the most dynamic segment of the system, characterized by strong hydrodynamic variability, sediment resuspension, and active reworking driven by tidal mixing processes. In contrast, the lower estuarine facies functions predominantly as a sediment accumulation zone, where reduced flow velocities promote deposition and the development of fine-grained deposits. The upper estuarine facies is largely transport-dominated, as low salinity conditions and limited flocculation reduce sediment cohesion, enhancing sediment mobility and downstream transport. These insights are supported by the observations of several authors who studied similar environments (Dalrymple et al., 1992; Winterwerp & van Kesteren, 2004).

4.6 Implications for Environmental Sustainability

The physicochemical characteristics and tidal dynamics of the Great Kwa River reveal a system that is presently stable but environmentally sensitive. The narrow ranges of temperature, pH, salinity, and conductivity indicate water quality conditions suitable for freshwater ecosystems. However, the observed

downstream gradients and facies transitions highlight the strong influence of tidal forcing and sediment reworking, which could be easily disrupted by anthropogenic activities or hydrological changes.

From a sustainability perspective, three key implications emerge:

4.6.1 Water Quality Preservation

The current physicochemical parameters fall within acceptable limits, but increasing salinity and conductivity downstream suggest potential vulnerability to saltwater intrusion, especially under scenarios of reduced fluvial discharge or climate-driven sea-level rise. Continuous monitoring is essential to safeguard water quality for ecological and human use.

4.6.2 Sediment Dynamics and Habitat Integrity

Turbidity and transparency patterns reflect localized sediment resuspension linked to channel morphology. Any alteration of flow regimes (e.g., dredging, sand mining, or dam construction) could intensify sedimentation, degrade habitats, and reduce biodiversity. Sustainable management must therefore regulate sediment extraction and maintain natural hydrodynamic processes.

4.6.3 Anthropogenic Sensitivity

Early signs of environmental sensitivity underscore the need for proactive management. Pollution from urban runoff, agricultural inputs, or industrial activities could rapidly alter ionic concentrations and turbidity, undermining ecological balance. Integrating community-based conservation with regulatory enforcement will be critical to maintaining sustainability.

Overall, the study provides a baseline for long-term environmental monitoring of tropical mesotidal rivers. By linking hydrodynamic controls to physicochemical variability, it emphasizes that sustainability in such systems depends on balancing natural tidal processes with responsible human activity. Effective management strategies should prioritize water quality monitoring, sediment regulation, and adaptive responses to climate change, ensuring that the Great Kwa River continues to support ecological integrity and human livelihoods.

4.7 Relevance to Coastal Conservation, Planning, and Management

The findings of this study have important implications for coastal conservation, environmental planning, and sustainable management of tropical estuarine systems within the Gulf of Guinea. The Great Kwa River forms part of the larger Cross River estuarine network and functions as a critical ecological and hydrological corridor supporting freshwater supply, sediment transport, fisheries, navigation, and biodiversity conservation. Understanding the interaction between tidal dynamics and physicochemical conditions therefore provides an essential scientific basis for evidence-based coastal management.

The delineation of hydro-physicochemical facies within the river highlights zones of varying environmental sensitivity and sedimentary behaviour. The middle transitional facies, characterized by active sediment reworking and elevated turbidity, represents a particularly dynamic zone that may be highly vulnerable to dredging, sand mining, shoreline modification, and infrastructure development. Identifying such sensitive zones is valuable for coastal zoning and environmental impact assessments, enabling planners to regulate anthropogenic activities in areas prone to ecological disturbance or geomorphic instability.

The observed downstream increase in salinity and conductivity also provides an early indication of potential saline intrusion pathways under changing hydrological conditions. This is especially relevant in the context of climate change and projected sea-level rise, which may intensify tidal penetration into freshwater systems. Consequently, the study offers baseline environmental data that can support adaptive coastal planning strategies aimed at protecting potable water resources, wetlands, and estuarine habitats from future salinization.

Furthermore, the study demonstrates that sediment transport and water quality in the Great Kwa River are strongly controlled by tidal asymmetry and channel morphology. These findings are directly applicable to river engineering, shoreline stabilization, dredging regulation, and sediment management programs. Maintaining natural hydrodynamic processes is essential for preserving channel stability, reducing excessive sedimentation, and sustaining habitat integrity within the estuarine system.

From a conservation perspective, the relatively stable physicochemical conditions observed in the river indicate that the system presently retains good ecological quality. However, increasing urbanization, industrial expansion, and catchment disturbance around Calabar may rapidly alter this balance if not properly managed. The study therefore emphasizes the importance of continuous environmental monitoring, integrated watershed management, pollution control, and community-based conservation initiatives as key components of sustainable coastal governance.

Overall, this research contributes valuable baseline information for integrated coastal zone management (ICZM) in southeastern Nigeria. By linking hydrodynamic behaviour with hydrochemical variability and sedimentary processes, the study provides a framework for predicting environmental change, guiding sustainable resource utilization, and improving resilience of tropical coastal systems under increasing anthropogenic and climatic pressures.

5. Conclusion

This study provides a comprehensive assessment of the physicochemical characteristics of the Great Kwa River and establishes clear linkages between hydrochemistry, tidal dynamics, and environmental sustainability within a tropical meso-tidal system. The river exhibits a semi-diurnal, ebb-dominated tidal regime, where the interaction between fluvial discharge and tidal forcing exerts a primary control on both hydrodynamic behavior and water quality distribution.

The physicochemical parameters—temperature (25–28°C), pH (6.0–7.5), salinity (0.014–0.039‰), electrical conductivity (20–58 µS/cm), and transparency (0.3–1 m)—fall within acceptable limits for freshwater systems, indicating that the Great Kwa River remains largely unpolluted and suitable for domestic use. The persistently low salinity confirms a freshwater-dominated tidal channel, despite its connectivity to the Cross River estuary, highlighting the dominance of fluvial input during the study period.

Distinct downstream gradients in salinity, conductivity, temperature, and pH reflect progressive tidal influence and incipient estuarine mixing. These gradients underpin the delineation of three hydro-physicochemical facies—upper (fluvial-dominated), middle (transitional), and lower (tidally influenced)—which collectively define the spatial organization of the river system. The middle facies emerges as the most dynamic zone, characterized by maximum variability in physicochemical conditions and active sediment reworking, while the lower facies serves as a zone of enhanced fine sediment deposition due to increased tidal influence and flocculation processes.

From a sedimentological perspective, the system exhibits a classic downstream facies succession from sandy fluvial deposits to heterolithic transitional units and mud-dominated estuarine facies. This organization is strongly governed by tidal asymmetry, salinity-induced flocculation, and channel bathymetry. Ebb dominance promotes net seaward sediment transport, reinforcing the role of the river as both a sediment conduit and a selective depositional environment.

Environmentally, the river system is relatively stable and supportive of aquatic life; however, emerging concerns such as localized turbidity maxima, slight downstream acidification, and increasing ionic concentrations suggest early signals of environmental stress. Given the river's strategic importance as a freshwater resource for Calabar and its vulnerability to anthropogenic pressures—including dredging, urban runoff, and potential saline intrusion—proactive management is essential.

In terms of environmental sustainability, the findings highlight the need for preventive action to safeguard water quality, regulate sediment dynamics, and mitigate anthropogenic impacts before stress signals escalate. The study establishes a critical baseline for adaptive monitoring and resource management, ensuring that the Great Kwa River continues to function as a resilient freshwater system and ecological corridor. Integrating these insights into regional coastal policies will be vital for balancing human use with ecological integrity in the Gulf of Guinea.

Overall, this study demonstrates that physicochemical dynamics in tidal rivers are tightly coupled with hydrodynamic processes and sedimentary regimes. The results not only enhance understanding of tropical meso-tidal systems but also provide a scientific framework for sustainable monitoring, conservation, and future environmental impact assessments in similar coastal settings.

6. Limitations of the Study

Despite providing important insights into the physicochemical dynamics and hydrodynamic controls of the Great Kwa River, this study has several limitations that should be considered when interpreting the results.

First, the study was conducted during the rainy season (August–September 2020) only. As a result, the observed physicochemical conditions primarily reflect wet-season hydrological processes characterized by high freshwater discharge and reduced saline intrusion. Seasonal variations associated with dry-season conditions, when tidal influence and salinity penetration may become more pronounced, were not evaluated. Consequently, the results represent a temporal snapshot rather than a full annual characterization of the river system.

Second, tidal current measurements were restricted to two monitoring stations along the channel. Although these stations captured the general ebb–flood dynamics of the river, they may not fully represent spatial variations in hydrodynamic behaviour across the entire estuarine system, particularly in zones affected by channel curvature, tributary inflow, or localized sediment accumulation.

Third, the study focused primarily on basic physicochemical parameters and hydrodynamic observations. Important environmental indicators such as dissolved oxygen, nutrients, chlorophyll concentration, suspended sediment concentration, heavy metals, hydrocarbons, and microbiological contaminants were not analyzed. Inclusion of these parameters would provide a more comprehensive assessment of ecosystem health and anthropogenic impact.

Another limitation relates to the absence of continuous long-term monitoring data. Parameters such as salinity, turbidity, and tidal velocity are highly dynamic and can vary significantly over tidal cycles, seasonal transitions, and extreme weather events. The lack of automated time-series measurements limits the ability to assess short-term variability and long-term environmental trends.

In addition, sedimentological interpretations were inferred largely from hydrodynamic and physicochemical patterns, supported by previous regional studies, rather than from direct sediment core analysis or laboratory grain-size characterization conducted concurrently with this investigation. Future studies integrating sediment cores, mineralogical analyses, and stratigraphic data would strengthen interpretations of facies development and sediment transport processes.

Finally, the study did not incorporate numerical hydrodynamic modelling or climate-change projections. Such approaches would improve understanding of future responses of the Great Kwa River to sea-level rise, altered freshwater discharge, dredging, and increasing anthropogenic pressure.

Notwithstanding these limitations, the study establishes an important baseline dataset for the Great Kwa River and provides valuable insights into the interactions between tidal dynamics, physicochemical variability, sedimentary processes, and environmental sustainability in tropical mesotidal systems.

Declarations

Ethics approval and consent to participate

This study did not involve human participants, human data, or animals. Therefore, ethical approval and consent to participate are not applicable.

Consent for publication

Not applicable.

Availability of data and materials

The datasets generated and/or analysed during the current study are available from the corresponding author on reasonable request. Where applicable, processed data supporting the findings of this study are included within the article.

Competing interests

The authors declare that they have no competing interests.

Funding

This research received no specific grant from funding agencies in the public, commercial, or not-for-profit sectors.

Authors' contributions

Conceptualization: Chimezie N. Emeka

Methodology: Chimezie N. Emeka, Victoria I. Emeka

Fieldwork and data collection: Chimezie N. Emeka, Victoria I. Emeka, Asukwo Essien Itam, Bassey Offiong Ekpo

Data analysis and interpretation: Chimezie N. Emeka, Victoria I. Emeka, Asukwo Essien Itam, Bassey Offiong Ekpo, Lailah Gifty Akita, Benjamin Odey Omang, Celsus Agim, Aniekan Clement Ukpe, Samuel Augustine Ikpe

Writing – Chimezie N. Emeka, Victoria I. Emeka

Writing – review and editing: Bassey Offiong Ekpo, Lailah Gifty Akita

Supervision: Etie Ben Akpan

All authors read and approved the final manuscript.

Acknowledgements

The authors acknowledge the support of the Institute of Oceanography, University of Calabar, for providing logistical assistance during fieldwork. We also appreciate the contributions of colleagues and field assistants who aided in sample collection and laboratory analyses.

References

1. Abascal-Zorrilla N, Vantrepotte V, Huybrechts N, Ngoc DD, Anthony EJ, Gardel A (2020) Dynamics of the estuarine turbidity maximum zone from Landsat-8 Data: the case of the Maroni River estuary, French Guiana. Remote Sens 12(13). https://doi.org/10.3390/rs12132173
2. Abril G, Riou SA, Etcheber H, Frankignoulle M, de Wit R, Middelburg JJ (2000) Transient, Tidal Time-scale, Nitrogen Transformations in an Estuarine Turbidity Maximum—Fluid Mud System (The Gironde, South-west France). Estuar Coast Shelf Sci 50(5):703–715. https://doi.org/10.1006/ecss.1999.0598
3. Allen GP, Salomon JC, Bassoulet P, Du Penhoat Y, De Grandpre C (1980) Effects of tides on mixing and suspended sediment transport in macrotidal estuaries. Sed Geol 26:69–90
4. Antia VI, Emeka CN, Ntekim EEU, Amah EA (2012) Grain size distribution and flow measurements in Qua-Iboe River estuary and Calabar Tidal River, S. E. Nigeria. Eur J Sci Res 67(2):223–239
5. Asp NE, Gomes VJC, Schettini CAF, Souza-Filho PWM, Siegle E, Ogston AS, Nittrouer CA, Silva JNS, Souza N Jr., Pereira SR, L. C. C., Queiroz MC (2018) Sediment dynamics of a tropical tide-dominated estuary: Turbidity maximum, mangroves and the role of the Amazon River sediment load
6. Aubrey DG (1986) Hydrodynamic controls on sediment transport in well-mixed bays and estuaries. In *Physics of Shallow Estuaries and Bays* (pp. 245–258). https://doi.org/10.1029/LN016p0245
7. Burchard H, Bolding K, Villarreal MR (2004) Three-dimensional modelling of estuarine turbidity maxima in a tidal estuary. Ocean Dyn 54(2):250–265. https://doi.org/10.1007/s10236-003-0073-4
8. Burchard H, Schuttelaars HM, Ralston DK (2018) Sediment trapping in estuaries. Annual Reviews Mar Sci 10:371–395. https://doi.org/10.1146/annurev-marine-010816-060535
9. Dalrymple RW (2010) Tidal depositional systems. In: James NP, Dalrymple RW (eds) Facies Models, vol 4. Geological Association of Canada

10. Dalrymple RW, Mackay DA, Ichaso AA, Choi KS (2012) Processes, Morphodynamics, and Facies of Tide-Dominated Estuaries. In *Principles of Tidal Sedimentology* (pp. 79–107). https://doi.org/10.1007/978-94-007-0123-6_5
11. Dalrymple RW, Zaitlin BA, Boyd R (1992) Estuarine facies models: conceptual basis and stratigraphic implications. J Sediment Petrol 62(6):1130–1146
12. Davies JL (1964) A morphogenic approach to world shorelines. Z für Geomorphologie 8(5):127–142. https://doi.org/10.1127/zfg/mortensen/8/1964/127
13. Davis RAJ, Dalrymple RW (2012) *Principles of tidal sedimentology* (R. A. J. Davis & R. W. Dalrymple, Eds.). Springer. https://doi.org/10.1007/978-94-007-0123-6
14. Dijkstra YM, Schuttelaars HM, Winterwerp JC (2018) The hyperturbid state of the water column in estuaries and rivers: the importance of hindered settling. Ocean Dyn 68:377–389. https://doi.org/10.1007/s10236-018-1132-1
15. Dyer KR, Christie MC, Manning AJ (2004) The effects of suspended sediment on turbulence within an estuarine turbidity maximum. Estuar Coast Shelf Sci 59(2):237–248. https://doi.org/10.1016/j.ecss.2003.09.002
16. Emeka CN, Antia VI, Ukpong AJ, Amah EA, Ntekim EEU (2010) A study on the sedimentology of tidal rivers: Calabar and Great Kwa, S. E. Nigeria. Eur J Sci Res 47(3):370–386
17. Emeka CN, Emeka VI, Agi-Odey E, Obim VN, Ambo A, Akita LG (2024a) Assessment of the rainy season physicochemical properties of the Qua-Iboe River estuary, southeast Nigeria. Int J Nat Appl Sci 17(1):47–51
18. Emeka CN, Emeka VI, Agi-Odey E, Obim VN, Ambo A, Akita LG (2024b) Physicochemical characteristics of the Calabar River, southeast Nigeria. Int J Nat Appl Sci 17(1):47–51
19. Emeka CN, Emeka VI, Agi-Odey EK, Ambo AA, Edem GO (2023) Wet season physicochemical characteristics of the Cross River estuary, Southeast, Nigeria. Global J Geol Sci 21:149–166. https://doi.org/10.4314/gjgs.v21i2.1
20. Emeka CN, Emeka VI, Akpan EB, Essien NU, Nwosu FM (2023) Dry season physicochemical characteristics of a tropical meso-tidal estuary: cross river estuary, southeast nigeria. Global J Geol Sci 21(2):183–200. https://doi.org/10.4314/gjgs.v21i2.3
21. Emeka CN, Emeka VI, Ebong ED, Ojong RA, Chidozie CP (2023) Dynamics in a tropical meso-tidal river: Great Kwa River, southeastern Nigeria (Gulf of Guinea). J Sediment Environ 8(4):617–633. https://doi.org/10.1007/s43217-023-00151-9
22. Emeka VI, Emeka CN, Agi-Odey E, Eteng SU, Itam AE, Akita LG (2024) Spatial variation of heavy metals in coastal waters of the Cross River estuary, southeast Nigeria. Int J Nat Appl Sci 17(1):52–59
23. Emeka VI, Emeka CN, Ebong ED, Ojong RA, Chikezie PC (2023) Tidal Dynamics And Physicochemical Parameters In A Tropical Estuary: Qua-Iboe River Estuary, Southeast Coast Of Nigeria. Global J Pure Appl Sci 29(2):175–192. https://doi.org/10.4314/gjpas.v29i2.8
24. Emeka VI, Emeka CN, Itam AE, Ambo A, Ukpe AC, Akita LG (2024) Heavy metal levels in coastal waters of a tropical estuary: Qua-Iboe River estuary, southeast Nigeria. Int J Nat Appl Sci 17(1):81–87
25. Emeka VI, Emeka CN, Itam AE, Nyong EE (2024) Factors influencing foraminiferal assemblages in coastal sediments of the Cross River Estuary, Southeast Nigeria, Gulf of Guinea. Discover Oceans 1(15):1–17. https://doi.org/10.1007/s44289-024-00017-6
26. Flemming BW (2012) Siliciclastic back-barrier tidal flats. In *Principles of Tidal Sedimentology* (pp. 231–267). https://doi.org/10.1007/978-94-007-0123-6_10
27. Freitas PTA, Silveira OFM, Asp NE (2012) Tide distortion and attenuation in an Amazonian tidal river. Brazillian J Oceanogr 60(4):429–446
28. Geyer WR, MacCready P (2014) The estuarine circulation. Annu Rev Fluid Mech 46(1):175–197. https://doi.org/10.1146/annurev-fluid-010313-141302
29. Ginsberg SS, Aliotta S Sediment transport circulation pattern through mesotidal channels system. In (pp. 23). IntechOpen.
30. Gong W, Schuttelaars H, Zhang H (2016) Tidal asymmetry in a funnel-shaped estuary with mixed semidiurnal tides. Ocean Dyn 66:637–658. https://doi.org/10.1007/s10236-016-0943-1
31. Grasso F, Bismuth E, Burchard H, Defontaine S, Kosters F, Lafite R, Reese L, Sottolichio A, van Kessel T, Vanlede J, van Maren DS, Walther R, Zorndt A (2025) Relating estuarine turbidity maxima to tide and river conditions. Sci Rep 16(1):1–11. https://doi.org/10.1038/s41598-025-32950-7
32. Guo L (2014) *Modelling estuarine morphodynamics under combined river and tidal forcing* [Ph.D. Delft University of Technology]. Delft
33. Guo L, van der Wegen M, Roelvink JA, He Q (2014) The role of river flow and tidal asymmetry on 1-D estuarine morphodynamics. J Geophys Research: Earth Surf 119:2315–2334. https://doi.org/10.1002/2014JF003110
34. Hayes MO (1979) Barrier island morphology as a function of tidal and wave regime. Academic
35. Hem JD (1985) Study and interpretation of the chemical characteristics of natural water. U.S. Geological Survey
36. Kaselowski T, Adams JB (2013) Not so pristine – characterising the physico-chemical conditions of an undescribed temporarily open/closed estuary. Water SA 39(5). https://doi.org/10.4314/wsa.v39i5.6
37. Li S, Gong C (2016) Flow dynamics and sedimentation of lateral accretion packages in sinuoud deep-water channels A 3D seismic case study from the northwestern South China Sea margin. J Afr Earth Sc 124:233–246
38. MacCready P, Geyer WR, Burchard H (2018) Estuarine Exchange Flow Is Related to Mixing through the Salinity Variance Budget. J Phys Oceanogr 48(6):1375–1384. https://doi.org/10.1175/jpo-d-17-0266.1
39. Matsoukis C, Amoudry LO, Bricheno L, Leonardi N (2022) Numerical Investigation of River Discharge and Tidal Variation Impact on Salinity Intrusion in a Generic River Delta Through Idealized Modelling. Estuaries Coasts 46(1):57–83. https://doi.org/10.1007/s12237-022-01109-2
40. Nichols G (2009) Sedimentology and stratigraphy. Wiley-Blackwell
41. Nigerian Navy (2018) *Tidal predictions for the Nigerian ports and river channels for the year 2018*

42. Odigie O, Obayagbona NO (2025) Saltwater Intrusion in Nigeria: A Review. Environ Technol Sci J 16(1):216–224. https://doi.org/10.4314/etsj.v16i1.22
43. Otogo GA, Asuquo FE, Agi-Odey EK (2021) Fluxes of physicochemical parameters in the Cross River Estuary, Nigeria. J Mar Sci Res Oceanogr 4(3):243–251
44. Park K, Wang HV, Kim S-C, Oh J-H (2008) A model study of the estuarine turbidity maximum along the main channel of the Upper Chesapeake Bay. Estuaries Coasts 31(1 223 7–007–90 1):115–133. https://doi.org/10.1 007/s
45. Reineck HE, Singh IB (1986) Depositional sedimentary environments: with reference to terrigenous clastics. Springer-. https://doi.org/10.1007/978-3-642-81498-3
46. Sexton WJ, Murday M (1994) The morphology and sediment character of the coastline of Nigeria-the Niger Delta. J Coastal Res 10(4):959–977
47. Ubuoh EA, Nwogu FU, Ossai-Abeh EQ, Ikwuemesi JC, Oke AO, Umoh JD (2024) Evaluation of hydro-chemical facies and surface water quality dynamics using multivariate statistical approaches in Southern Nigeria. Sci Rep 1–26. https://doi.org/10.1038/s41598-024-77534-z
48. Ukpong AJ, Ikediasor CK, Emeka CN, Emeka VE (2015) Tidal influence on foraminifera distribution in a typical mesotidal river; a case study of the Great Kwa River, southeastern Nigeria. Int J Sci Eng Res, *6*(7)
49. Uncles RJ (2002) Estuarine Physical Processes Research: Some Recent Studies and Progress. Estuar Coast Shelf Sci 55(6):829–856. https://doi.org/10.1006/ecss.2002.1032
50. Uncles RJ, Stephens JA, Harris C (2006) Properties of suspended sediment in the estuarine turbidity maximum of the highly turbid Humber Estuary system, UK. Ocean Dyn 56(3–4):235–247. https://doi.org/10.1007/s10236-005-0053-y
51. Whitehouse R, Soulsby R, Roberts W, Mitchener H (2000) Dynamics of estuarine muds: a manual for practical applications. Thomas Telford
52. Winterwerp JC (2007) On the sedimentation rate of cohesive sediment. Estuar Coastal Fine Sediments Dynamics, 209–226
53. Winterwerp JC, van Kesteren WGM (2004) *Introduction to the physics of cohesive sediment in the marine environment* (1 ed., Vol. 56). Elservier
54. Winterwerp JC, Wang Z-B (2021) Hydrosedimentological response to estuarine deepening conceptual analysis. J Waterway Port Coastal Ocean Eng 147(5):04021023–0402102104021023. https://doi.org/10.1061/(ASCE)WW.1943-5460.0000660
55. Winterwerp JC, Wang ZB, van Braeckel A, van Holland G, Kösters F (2013) Man-induced regime shifts in small estuaries—II: a comparison of rivers. Ocean Dyn 63(11–12):1293–1306. https://doi.org/10.1007/s10236-013-0663-8
56. World Health Organization (2011) Guidelines for drinking-water quality, Fourth edn. World Health Organisation
57. World Health Organization (2017) Guidelines for drinking-water quality, Fourth edn. World Health Organization
58. World Health Organization (2022) Guidelines for drinking-water quality, Fourth edn. World Health Organization

Figures

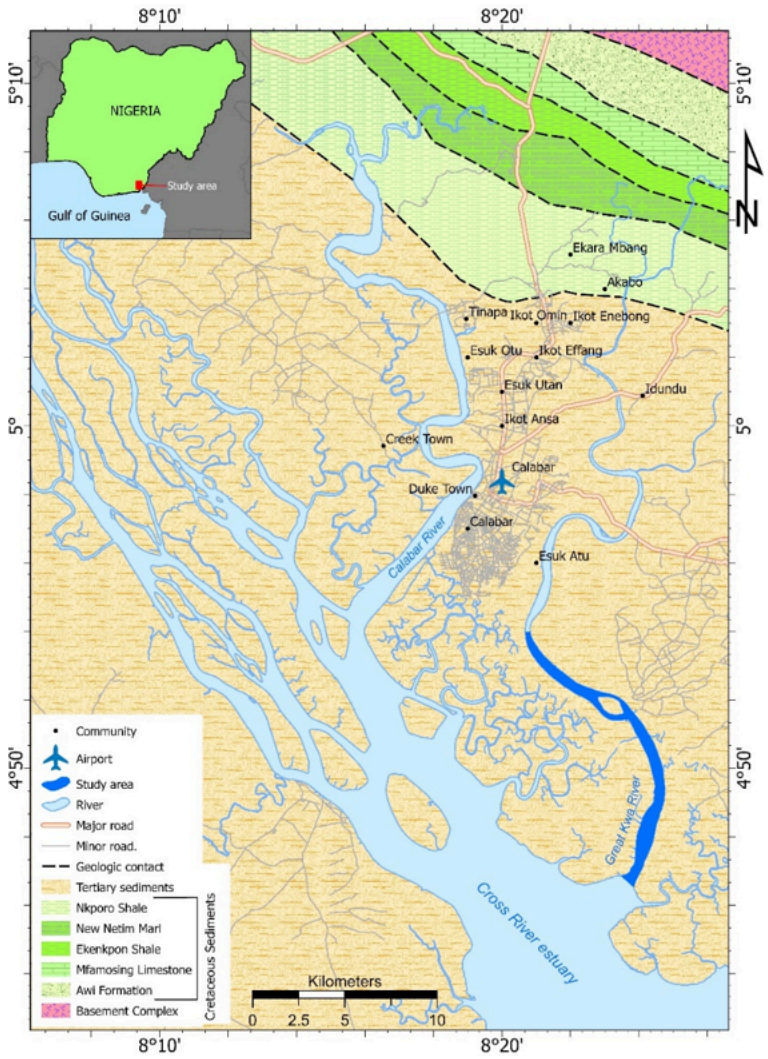


Figure 1

Map of the Cross River estuary system showing the studied segment of Great Kwa River and the geology of the environs

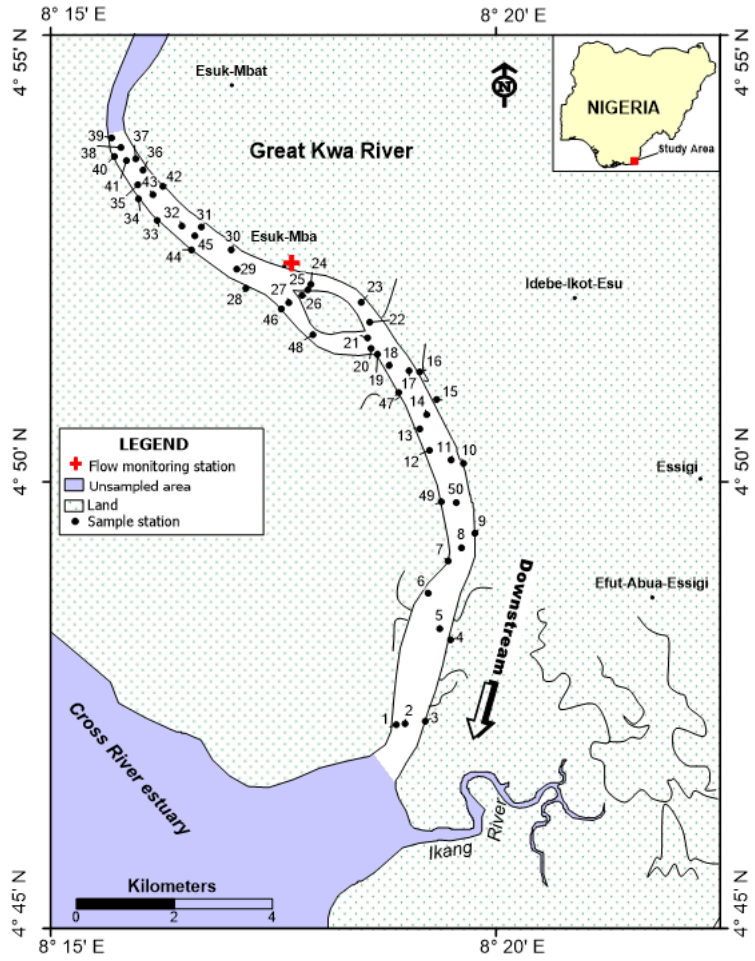


Figure 2

Great Kwa River sample distribution map

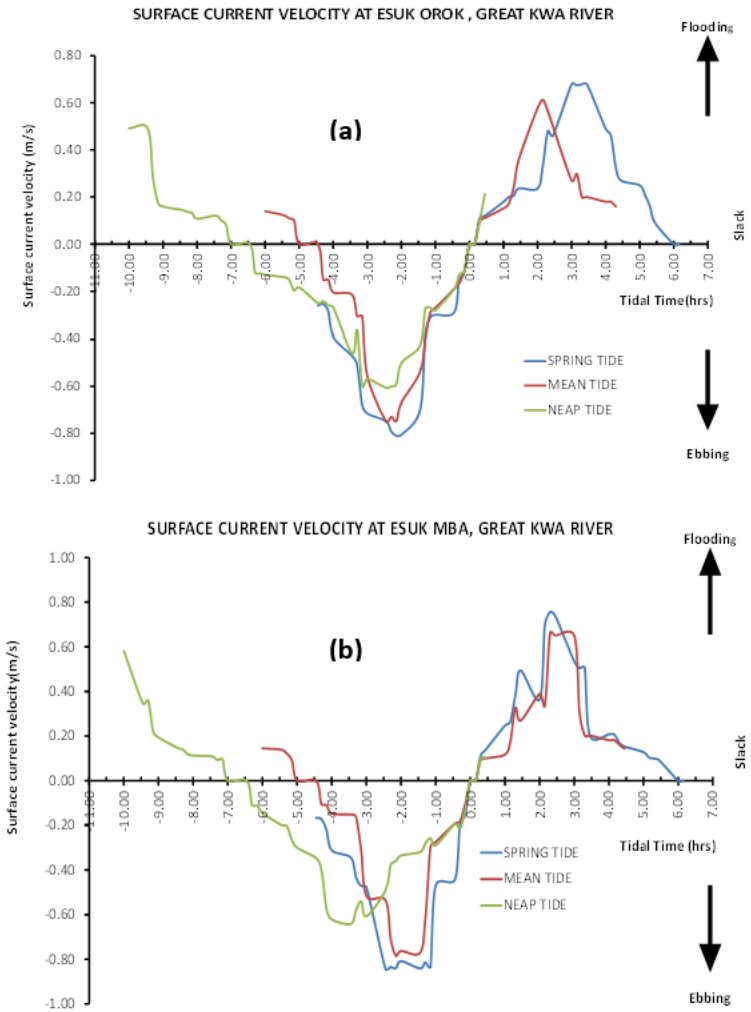


Figure 3

Surface tidal current velocity at Great Kwa River (a) Esuk Orok (Spring tide, Mean tide, and Neap tide) and (b) Esuk Mba (Spring tide; Mean tide; and Neap tide)

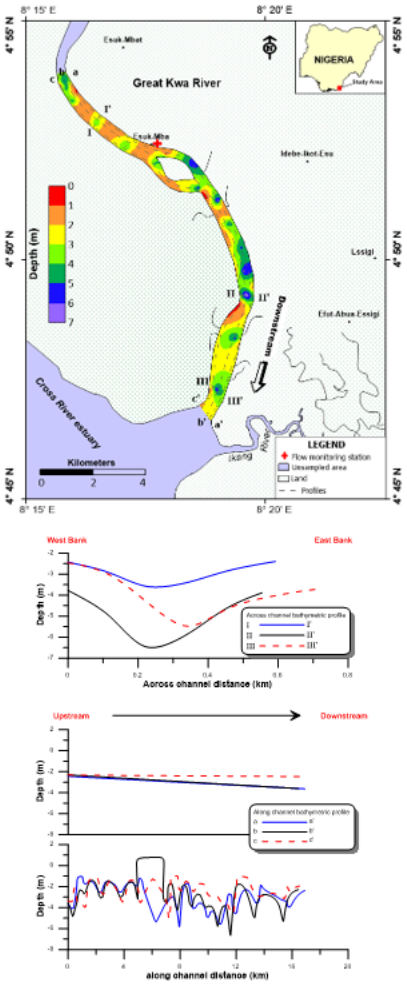


Figure 4

(a) Bathymetric map of Great Kwa River relative to mean tide low water slack (b) across channel sections (c) resolved along channel linear trends (d) along channel sections

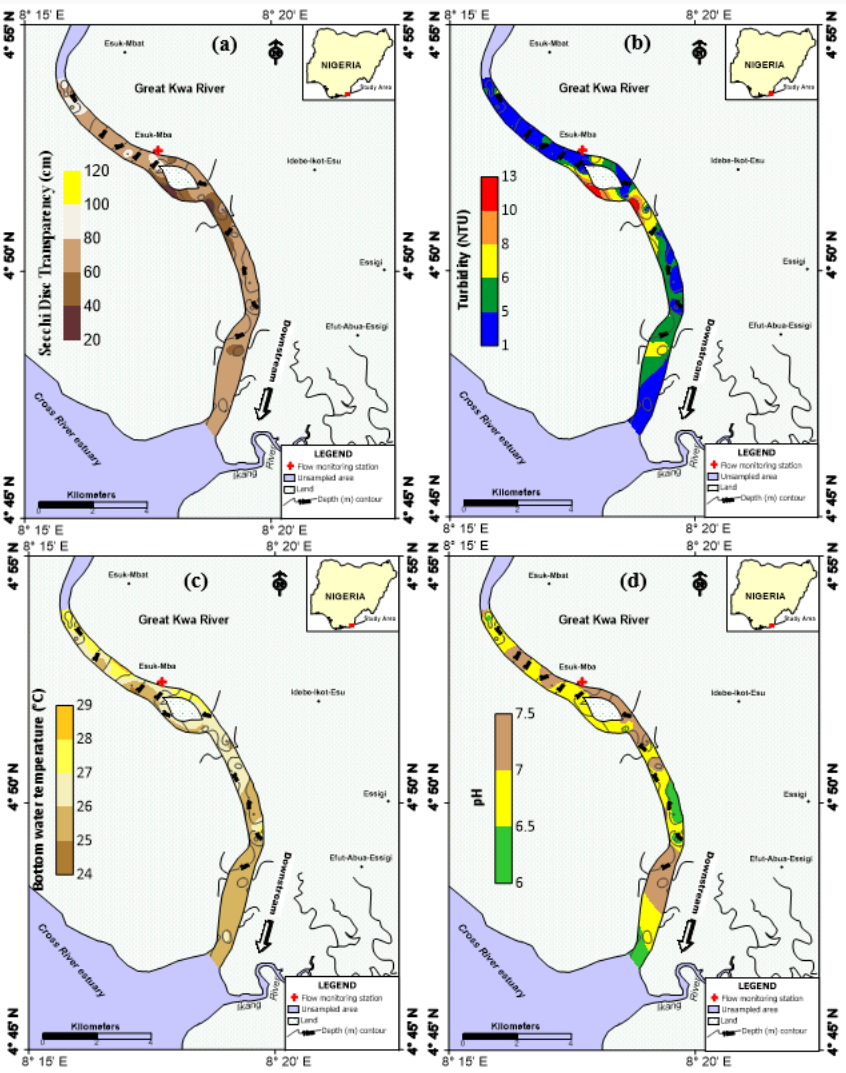


Figure 5

Spatial distribution of (a) Secchi disc transparency, (b) turbidity, (c) bottom water temperature, and (d) pH, in Great Kwa River

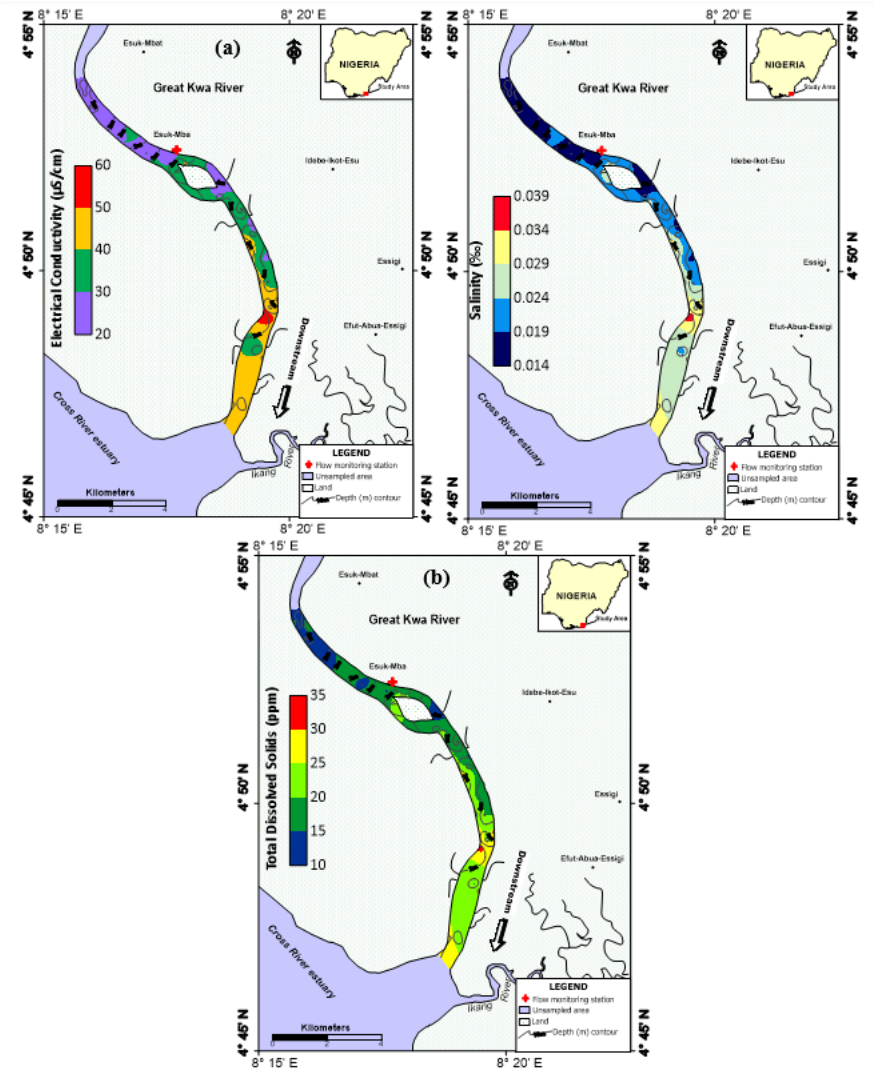


Figure 6

Spatial distribution of bottom water (a) electrical conductivity (b) salinity, and (c) total dissolved solids in Great Kwa River

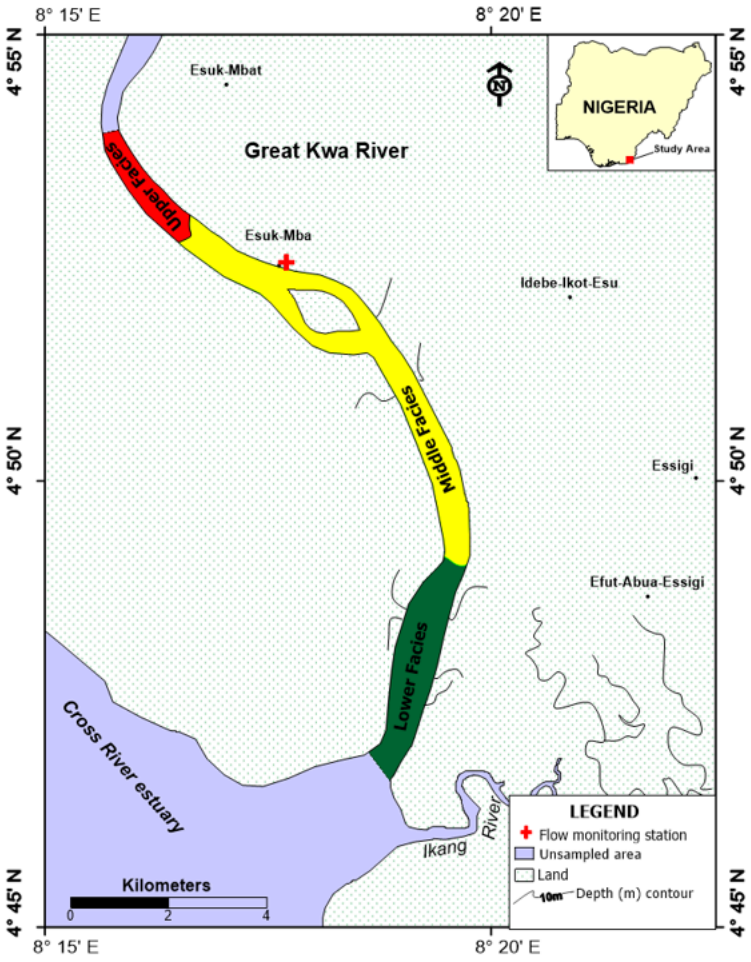


Figure 7

Hydro-physicochemical facies of the Great Kwa River